Table 1 Control parameters for $r = 1.5$

τ_f	Optimal fuel	τ_j	sgn$[g(\eta^*, \tau_j)]$	c_j
4.0	6.5940863	0.0000000	−	0.1135749
		1.0622951	+	0.2882963
		2.9377049	−	0.3623254
		4.0000000	+	0.2358035
6.0	1.5501346	0.2297864	+	0.4366778
		3.3180872	−	0.1137695
		6.0000000	+	0.4483121
8.0	1.5000000	0.0000000	+	0.5000000
		3.1415927	−	0.0000000
		6.2831853	+	0.5000000
10.0	1.5000000	0.0000000	+	0.0000000
		3.1415927	−	0.5000000
		6.2831853	+	0.0000000
		9.4247780	−	0.5000000

rapid maneuver, which is characterized by high fuel consumption. This maneuver requires four impulses of different magnitudes. Three impulses of different magnitudes are required for $\tau_f = 6$. The optimal fuel required for this case is close to the minimum achieved for $\tau_f \geq 2\pi$. In contrast, only two impulses are required when $\tau_f = 8$, with the optimal fuel consumption equal to the minimum possible consumption. Further increases in τ_f offer no advantage in fuel consumption for this case. However, for large τ_f there may exist multiple solutions to the selection of impulse coefficients, enabling flexibility in the optimal control system design. For example, an infinite number of pulsing schemes are possible for the case $\tau_f = 10$. The coefficients contained in Table 1 were chosen such that the control requires only one-sided pulsing. This control is demonstrated in Fig. 3. A pulse applied at $\tau = \pi$ yields a step change in $\dot{\psi}$, exciting the precessional motion of the body. A second pulse applied at $\tau = 3\pi$ terminates the precessional motion and completes the desired reorientation maneuver.

IV. Conclusion

A recently developed numerical technique for exactly solving fuel optimal control problems has been demonstrated on a classical problem. The adaptive grid bisection search was discussed and applied to the problem of fuel optimal reorientation of axisymmetric spin-stabilized rigid satellites. This approach was shown to be useful in determining the fuel optimal impulsive control strategy, particularly when rapid maneuvers are desired. For large enough maneuver times, the method produced the familiar two-impulse reorientation maneuver. For even larger maneuver times, the existence of multiple optimal pulsing schemes was revealed.

Acknowledgments

This research was supported by NASA Grant NAGW-1331 to the Mars Mission Research Center and by NASA Grant NAG1-977 monitored by Raymond Montgomery. The authors wish to express their gratitude to E. N. Chukwu for his continued assistance.

References

[1]Grubin, C., "Generalized Two-Impulse Scheme for Reorienting a Spin Stabilized Vehicle," *Progress in Astronautics and Rocketry, ARS, Guidance and Control,* Vol. 8, 1962, Academic, New York, pp. 649–668.

[2]Porcelli, G., and Connolly, A., "Optimal Attitude Control of a Spinning Space-Body—A Graphical Approach," *IEEE Transactions on Automatic Control,* Vol. AC-12, No. 3, 1967, pp. 241–249.

[3]Yin, M., and Grimmell, W. C., "Optimal and Near-Optimal Regulation of Spacecraft Spin Axis," *IEEE Transactions on Automatic Control,* Vol. AC-13, No. 1, 1968, pp. 57–64.

[4]Wingate, R. T., "Fuel-Optimal Reorientation of a Spinning Body," Ph.D. Dissertation, Dept. of Engineering Mechanics, Virginia Polytechnic Inst. and State Univ., Blacksburg, VA, July 1970.

[5]Krasovskii, N. N., "On the Theory of Optimal Control," *Journal of Applied Mathematics and Mechanics,* Vol. 23, No. 4, 1959, pp. 899–919.

[6]Neustadt, L. W., "Minimum Effort Control Systems," *SIAM Journal on Control,* Vol. 1, No. 1, 1962, pp. 16–31.

[7]Redmond, J., and Silverberg, L., "Fuel Consumption in Optimal Control," *Journal of Guidance, Control, and Dynamics,* Vol. 15, No. 2, 1992, pp. 424–430.

[8]Silverberg, L., and Redmond, J., "Fuel Optimal Reboost of Flexible Spacecraft," AIAA/ASME/ASCE/AHS/ASC 33rd Structures, Structural Dynamics, and Materials Conference (Dallas, TX), April 13–15, 1992 (AIAA Paper 92-9086); also *Journal of Guidance, Control, and Dynamics* (to be published).

Ground Verification for Satellite High-Accuracy Onboard Antenna Drive Control Systems

Hiroshi Tanaka* and Yoichi Kawakami†

NTT Radio Communication Systems Laboratories, Kanagawa-ken 238-03, Japan

Nomenclature

F = suspension force of wire
G = gravity center of rotation part [antenna pointing mechanism (APM) rotor and inertia dummy]
K = rigidity of the APM rotation in gravity compensation
k = rigidity of the APM bearings rotation
N = drive torque of the actuator in the APM
P = suspension point by wire
T_{az} = torque around azimuth axis
T_{el} = torque around elevation axis
W = weight of the rotation part
W_G = weight of the azimuth gimbal and the elevation gimbal
Z = distance between the azimuth axis and point G
Z_G = distance between azimuth axis and elevation axis
Z_P = distance between point G and point P
α = rotation angle around azimuth axis
β = rotation angle around elevation axis

Introduction

In multibeam satellite communication systems, it is necessary for the beam pointing direction of the onboard antennas to be accurately controlled because of their narrow beamwidth. An antenna drive control system (ADCS), which drives the antenna's reflector, has been developed to satisfy the pointing accuracy requirement.[1,2] Since this onboard control system operates in a space orbit, it is important to carry out ground tests under a simulated space environment in order to precisely verify the control characteristics. However, the trend toward large antennas makes it quite difficult to simulate the space

Presented as Paper 91-487 at the AAS/AIAA Astrodynamics Conference, Durango, CO, Aug. 19–22, 1991; received Sept. 2, 1991; revision received April 3, 1992; accepted for publication April 7, 1992.

*Research Engineer.

†Senior Research Engineer, Supervisor.

environment and to implement a closed-loop test system using actual reflectors.

This Note presents methods to ground verify the control characteristics. A gravity compensation method is investigated, and a closed-loop test system is implemented by using newly developed test equipment. After the validity of the designed ground test system is confirmed, the control error of the ADCS for the Japanese Engineering Test Satellite (ETS-VI) is verified.

Ground Test System

Gravity Compensation

The basic configuration of the ADCS is shown in Fig. 1. It consists of an RF sensor, antenna pointing electronics (APE), and an APM. The function of the ADCS is to compensate the antenna pointing errors detected by the RF sensor by rotating the reflector installed on the APM around two orthogonal axes. Since the generation torque of the APM has been minimized, it cannot be tested unless the effect of gravity is eliminated or offset. A gravity condition of $\sim 10^{-4}g$ (where g represents the acceleration of gravity on the ground) was assumed from the maximum acceleration of a 2 ton-class geostationary satellite due to the operation of thrusters. An inertia dummy representing the reflector was attached to the APM. The gravity compensation method is shown in Fig. 1. The torque expressions are derived from the torque balance around the rotation axes:

$$T_{az} = \left[(F - W)Z - FZ_P\right]\sin\alpha\cos\beta \tag{1}$$

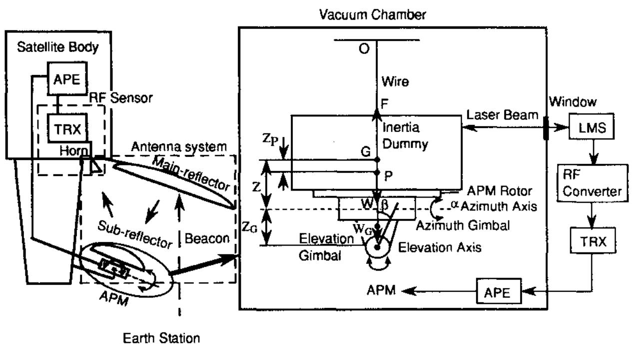

Fig. 1 Onboard configuration and test system configuration.

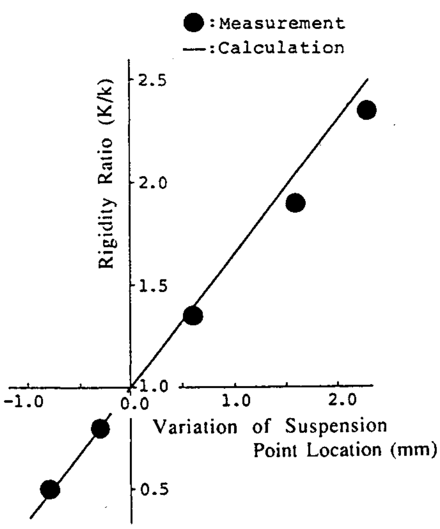

Fig. 2 Variation of suspension point location and rigidity ratio.

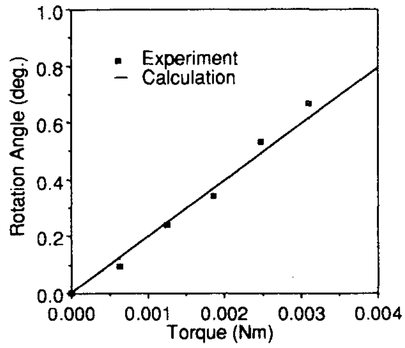

Fig. 3 Drive torque and rotation angle.

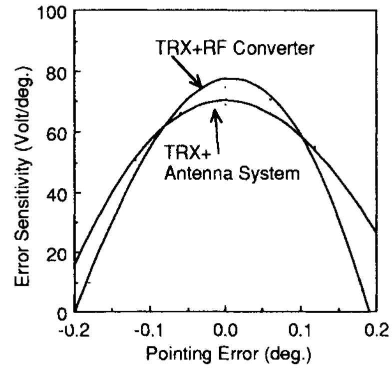

Fig. 4 RF sensor simulation obtained with RF converter.

$$T_{el} = \left[(F - W)Z - FZ_P\right]\cos\alpha\sin\beta + \left[(F - W)Z_G - \tfrac{1}{2}W_G Z_G\right]\sin\beta \tag{2}$$

It is assumed that the gravity center of the azimuth and elevation gimbal is at the midpoint between both gimbals and the suspension force opposes gravity. To eliminate these torques, which are regarded as compensation errors, the following conditions are obtained:

$$F = (2W + W_G)/2 \tag{3}$$

$$Z_P = W_G Z/(2W + W_G) \tag{4}$$

This method was confirmed using the APM (Ref. 3) of the ADCS for the ETS-VI. The rotor and the stator of this APM were linked with elastic bearings, whose rotation angles were proportional to the applied torques. We can substitute $Z_G = 0$ from the APM structure. The APM rotation angles α and β are small (maximum of 1 deg). Therefore, the following expressions were obtained:

$$\left[k + (F - W)Z - FZ_P\right]\alpha = N \tag{5}$$

$$K \equiv \left[k + (F - W)Z - FZ_P\right] \tag{6}$$

K was introduced to evaluate compensation accuracy. Rigidity of the APM rotation is considered to be k in zero gravity. The difference between K and k is taken as the compensation error. Since the suspension force F can be set at W measured, the compensation error can be made to approach zero by adjusting the location of P with reference to k obtained from the bearing test.

Figure 2 shows the relationship between the location of P and the rigidity ratio (K/k). K was calculated from the APM rotation angle measurements and N generated. It was con-

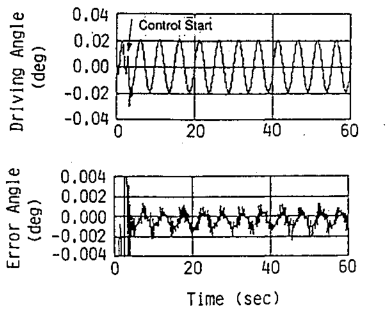

Fig. 5 Control accuracy of the ADCS.

firmed that the rigidity ratio was proportional to the location of P and a ratio of 1 can be achieved (i.e., $K = k$).

Figure 3 shows the relationship between the drive torque and the APM rotation angles after appropriate adjustment of the location of P with a resolution of ~ 0.05 mm. A K of 4.57×10^{-3} Nm/deg was obtained from the experimental data, and the solid line indicates k (5.06×10^{-3} Nm/deg). It was confirmed that the maximum torque due to compensation error could be suppressed to less than 4.9×10^{-4} Nm. When mZ (where m represents mass of the rotation part) is equal to 0.3 kg, which is obtained from the ADCS parameters of the ETS-VI, the error is considered to be equivalent to a $1.7 \times 10^{-4} g$ environment.

Closed-Loop Test System

The right part of Fig. 1 shows the closed-loop test system. Two orthogonally positioned laser measurement systems (LMSs), whose resolution was less than 0.0001 deg, were used considering the ADCS control accuracy to be verified. The laser beams were transmitted through windows in the chamber. The RF converter was developed to reproduce the RF signals generated by the antenna system. The sensitivity for the pointing error obtained with the RF converter and that obtained with the RF sensor were compared to evaluate the simulation accuracy. The result is shown in Fig. 4. It was verified that the gain variation of ADCS is only ~ 1 dB.

The test system was used to confirm the ADCS for the ETS-VI and measure its control error. The results are shown in Fig. 5. The upper graph is the pointing movement corresponding to the attitude change, and the lower graph indicates the control error. It was verified that the ADCS achieves the required accuracy of ~ 0.002 deg.

Conclusion

This Note outlines ground verification methods for onboard antenna drive control systems to ground verify control characteristics in orbit. Gravity compensation by adjusting the suspension point location was proposed, and its accuracy was confirmed by experiments. A closed-loop test system was developed and applied to the ADCS to verify its control accuracy.

References

[1]Bittner, H., Brauch, A., Bruderle, C., Roche, A., Starke, J., and Surauer, M., "The Attitude and Orbit Control Subsystem of the TV-SAT/TDF1 Spacecraft," *Proceedings of the Ninth IFAC/ESA Symposium on Automatic Control in Space* (Noordwijkerhout, The Netherlands), July 1982, pp. 83–102.

[2]Kawakami, Y., Hojo, H., and Ueba, M., "Design of an On-Board Antenna Pointing Control System for Communication Satellite," *Proceedings of the AIAA/AAS Astrodynamics Conference* (Minneapolis, MN), Aug. 1988, pp. 689–694 (AIAA Paper 88-4306-CP).

[3]Tsukada, E., Kawakami, Y., Miyake, S., and Ogawa, S., "On-Board Antenna Pointing Mechanism for Multi-Beam Satellite Communication Systems," *Japan Society of Mechanical Engineers International Journal,* Vol. 30, No. 270, 1987, pp. 2011–2017.

Elastomer Damper for a Freely Precessing Dual-Spin Seeker

C. O. Chang* and M. P. Chen†
National Taiwan University,
Taipei 107, Taiwan, Republic of China

Introduction

THE dual-spin seeker as shown in Fig. 1 is typical of a gyro-optical system used in the guidance of radiation seeking missiles. By rotating the purposefully nonaligned scanning mirrors at different angular rates, a rosette scanning pattern is generated. A significant virtue of the rosette lies in the fact that the maximum information sampling of the pattern exists at the center of the pattern. This characteristic renders the system inherently less sensitive to the effects of spurious targets.[1] The two mirrors are fully gimbaled for tracking a target. A nutation damper is mounted on the post that is fixed in the inner gimbal. The center of gravity of the dual-spin seeker is located at the point O, which is also the intersection point of the rotating axes of the inner and outer gimbals.

When the primary rotor is subjected to an impulsive torque, i.e., a suddenly applied torque of brief duration, coning motion of its spin axis about the angular momentum vector (which is fixed in space in the absence of external torques) will occur. For the purpose of positioning, this coning motion must be suppressed. The commonly used damping devices for removing the coning motion of satellites are viscous fluid dampers.[2] Martin[3] commented that an elastomer damper is better than a viscous fluid damper from the viewpoint of stability. The damping performance of the elastomer damper, consisting of a viscoelastic cantilever beam with a tip rigid body attached at its free end, is analyzed in this Note. For simplicity, we neglect the effect of gimbals and then the model of a double-gimbaled dual-spin seeker is basically the same as that previously adopted for dual-spin spacecraft. The gyroscopic seeker is modeled as two symmetric bodies with the same spin axis as shown in Fig. 2. The $OXYZ$ coordinate system is a fixed inertial frame. The origin O coincides with the center of mass of the two-body system. The $Ox_p y_p z_p$ coordinate system is fixed in the outer gimbal with the y_p axis passing through the axis of the gimbal bearing. The angular displacement of the x_p axis with respect to the X axis is denoted by ϕ. The $Ox_n y_n z_n$ coordinate system is fixed in the inner gimbal with the x_n axis passing through the inner gimbal bearing. The angular displacement of the y_n axis measured from the y_p axis is denoted by θ. The spin rate of the primary rotor is denoted by $\dot{\psi}$, and the spin rate of the secondary rotor is $\alpha\dot{\psi}$ where α is a constant.

The model of the elastomer damper is shown in Fig. 2b. The longitudinal direction of the short viscoelastic beam is parallel to the x_n axis. The purposes of the tip body are to enhance the vibration of the beam to speed up the absorption of the energy of coning motion and to provide a degree of freedom for tuning the frequency of the damper by properly choosing the mass of the tip body. Two different viscoelastic materials, the Kelvin-Voigt and the three-parameter materials, of which the beam is made, are considered in this Note.

Kelvin-Voigt Elastomer Damper

Let $\boldsymbol{e}_1$, $\boldsymbol{e}_2$, and $\boldsymbol{e}_3$ be the unit vectors of the x_n, y_n, and z_n axes. The angular velocities of the primary and secondary rotors are $\omega_p = \dot{\theta}\boldsymbol{e}_1 + \dot{\phi}\cos\theta\boldsymbol{e}_2 + (\dot{\psi} - \dot{\phi}\sin\theta)\boldsymbol{e}_3$

Received Oct. 9, 1990; revision received Dec. 13, 1991; accepted for publication Jan. 10, 1992.

*Associate Professor, Institute of Applied Mechanics.
†Graduate Student.